Published in "Current Biology 26(5): 661–669, 2016"
which should be cited to refer to this work.

Four Individually Identified Paired Dopamine Neurons Signal Reward in Larval *Drosophila*

Astrid Rohwedder,[1,2] Nana L. Wenz,[2] Bernhard Stehle,[2] Annina Huser,[2] Nobuhiro Yamagata,[3] Marta Zlatic,[4] James W. Truman,[4] Hiromu Tanimoto,[3] Timo Saumweber,[5,*] Bertram Gerber,[5,6,7,*] and Andreas S. Thum[1,2,8,*]
[1]Department of Biology, University of Fribourg, 1600 Fribourg, Switzerland
[2]Department of Biology, University of Konstanz, 78464 Konstanz, Germany
[3]Graduate School of Life Sciences, Tohoku University, Katahira 2-1-1, 980-8577 Sendai, Japan
[4]Janelia Research Campus, Ashburn, VA 20147, USA
[5]Abteilung Genetik von Lernen und Gedächtnis, Leibniz Institut für Neurobiologie (LIN), 39118 Magdeburg, Germany
[6]Otto von Guericke Universität Magdeburg, Institut für Biologie, Verhaltensgenetik, Universitätsplatz 2, 39106 Magdeburg, Germany
[7]Center for Behavioral Brain Sciences (CBBS), 39106 Magdeburg, Germany
[8]Zukunftskolleg, University of Konstanz, 78464 Konstanz, Germany
*Correspondence: timo.saumweber@lin-magdeburg.de (T.S.), bertram.gerber@lin-magdeburg.de (B.G.), andreas.thum@uni-konstanz.de (A.S.T.)

SUMMARY

Dopaminergic neurons serve multiple functions, including reinforcement processing during associative learning [1–12]. It is thus warranted to understand which dopaminergic neurons mediate which function. We study larval *Drosophila*, in which only approximately 120 of a total of 10,000 neurons are dopaminergic, as judged by the expression of tyrosine hydroxylase (TH), the rate-limiting enzyme of dopamine biosynthesis [5, 13]. Dopaminergic neurons mediating reinforcement in insect olfactory learning target the mushroom bodies, a higher-order "cortical" brain region [1–5, 11, 12, 14, 15]. We discover four previously undescribed paired neurons, the primary protocerebral anterior medial (pPAM) neurons. These neurons are TH positive and subdivide the medial lobe of the mushroom body into four distinct subunits. These pPAM neurons are acutely necessary for odor-sugar reward learning and require intact TH function in this process. However, they are dispensable for aversive learning and innate behavior toward the odors and sugars employed. Optogenetical activation of pPAM neurons is sufficient as a reward. Thus, the pPAM neurons convey a likely dopaminergic reward signal. In contrast, DL1 cluster neurons convey a corresponding punishment signal [5], suggesting a cellular division of labor to convey dopaminergic reward and punishment signals. On the level of individually identified neurons, this uncovers an organizational principle shared with adult *Drosophila* and mammals [1–4, 7, 9, 10] (but see [6]). The numerical simplicity and connectomic tractability of the larval nervous system [16–19] now offers a prospect for studying circuit principles of dopamine function at unprecedented resolution.

RESULTS AND DISCUSSION

Four Paired Tyrosine-Hydroxylase-Positive Neurons of the Previously Undescribed pPAM Cluster Innervate the Larval Mushroom Body

Judged by the defects of dopamine receptor mutants, the dopaminergic system is necessary for aversive and appetitive olfactory learning [5]. However, although it was revealed that aversive learning can come about by dopaminergic cells covered by the TH-Gal4 driver, including those of the DL1 cluster [5], the cellular identity of neurons involved in appetitive learning of the larva remained clouded. We aimed to reveal the nature of these cells.

We use an antibody that specifically recognizes the enzyme tyrosine hydroxylase (TH) to identify neurons as likely to be dopaminergic [5, 20], as the TH enzyme specifically catalyzes the rate-limiting step of dopamine biosynthesis. We confirm the three previously reported cell clusters (DL1, DL2, and DM; Figure 1A) [5, 20–22]. We additionally uncover a cluster located anteriorly and medially, consisting of four pairs of TH-positive neurons (Figures 1B–1I). We termed this cluster the primary-lineage protocerebral anterior medial (pPAM) cluster and the respective neurons pPAM1–4. This cluster is not evident in the larval TH-Gal4 expression pattern and had therefore previously escaped attention (in flp-out experiments from TH-Gal4, only a faint expression in pPAM2 was rarely observed [5]).

We then screened the larval expression patterns of the Janelia collection of Gal4 driver strains [23] for coverage of pPAM neurons and identified the strains R30G08, R58E02, and R64H06 (Figures 2 and S1). These driver strains show specific expression in two, three, and four pPAM neurons, respectively, per brain hemisphere (Figures 2A–2I and S1). Analyses of flp-out expression patterns [24] for each strain show that R30G08 covers the pPAM1,3 neurons, whereas R58E02 expresses in pPAM1,3,4 and R64H06 in all four pairs of pPAM cluster neurons (Figure S1). These pPAM neurons innervate the mushroom body medial lobe at four distinct tiles (Figures 1E–1I and S1). The flp-out experiments also showed rare expression in the pPAM2 neuron in the R30G08 and R58E02 driver strains (4 out of 97 brains; boxed

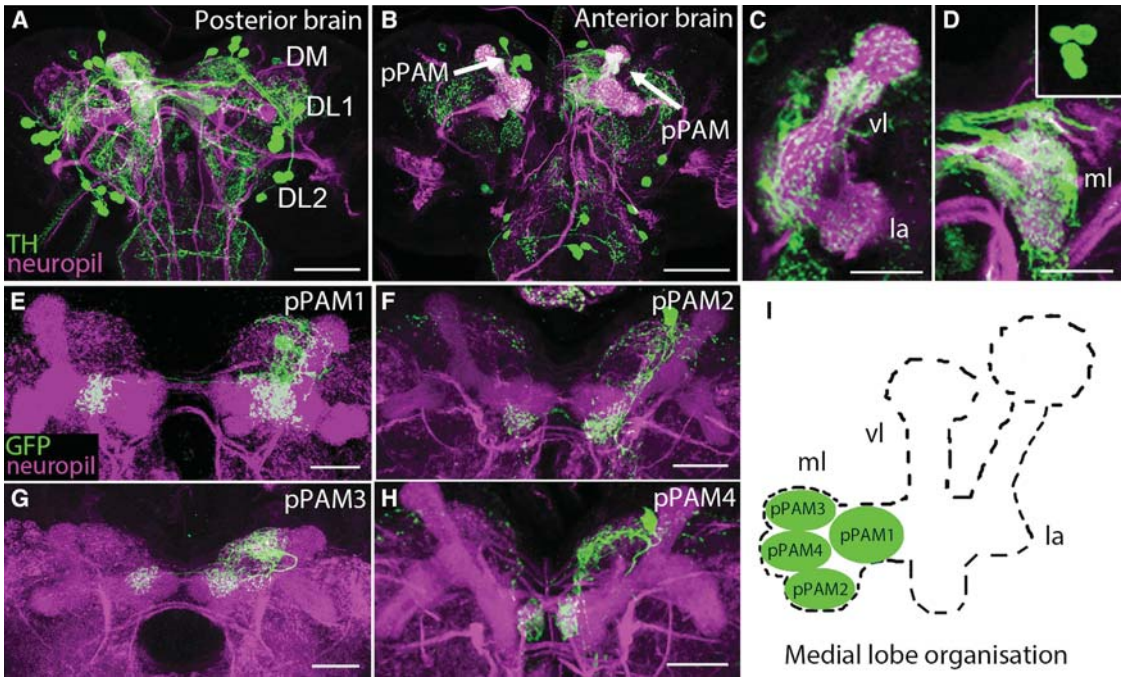

Figure 1. Four Paired Neurons, pPAM1–4, Subdivide the Mushroom Body Medial Lobes into Four Distinct Tiles

(A–D) Anti-TH labeling shows likely dopaminergic neurons (green), and anti-ChAT/FasII staining reveals the neuropil/axonal tracts (magenta) of partial brain projections from TH-Gal4;UAS-*mCD8::GFP* larvae.

(A) In the posterior half of the brain, the three previously identified clusters of TH-positive neurons called DL1, DL2, and DM can be discerned.

(B) In the anterior half of the brain, a paired cluster of four TH-positive neurons is here identified and named primary-lineage protocerebral anteriormedial cluster (pPAM1–4, arrows).

(C and D) TH-positive neurons densely innervate the mushroom body, including its vertical lobe (vl), lateral appendix (la), and medial lobe (ml) (only the right brain hemisphere is shown; the insert in D shows the four cell bodies of the mushroom body-projecting pPAM neurons).

(E–H) Flp-out clones of Gal4 strains (see Figure 2) that cover the pPAM cluster reveal distinct innervation in the tiles of the mushroom body medial lobe, symmetrically for both hemispheres. Green labeling shows anti-GFP staining; magenta labeling is as above. For a more detailed anatomical description, see Figure S1.

(I) Schematic of the tiled organization of the medial lobe of the right brain hemisphere and the innervation by the pPAM1–4 neurons.

Scale bars, 50 μm (A and B) and 25 μm (C–H). See also Figure S1.

in gray in Figure S1). Across the large number of animals involved in behavioral testing, though, such low-probability expression would be without measurable consequence [25].

Using the dendritic marker DenMark to reveal postsynaptic regions [26] and Synaptobrevin-GFP to label presynaptic regions [27], we found that presynaptic staining from pPAM cluster neurons was detectable in the medial lobe and postsynaptic labeling across the lateral and medial protocerebrum and weakly in the medial lobe (Figures 2J–2O).

Taken together, these data suggest that the four paired pPAM neurons deliver a likely dopaminergic signal to the medial lobe of the mushroom body and do so individually for separate mushroom body lobe tiles.

pPAM Neurons Acutely Function for Appetitive, but Not Aversive, Learning

We crossed the driver strains R30G08, R58E02, and R64H06 for the expression of the apoptosis proteins Hid and Reaper to ablate [28, 29] the respective sets of pPAM neurons (Figures S4A and S4B). These animals were then tested in an odor-sugar associative memory paradigm [30]. As sugars we used fructose, arabinose, and sorbitol [31, 32], as they differ in nutritional value and thus conceivably in the set of sensory neurons that they activate.

Ablation of only the pPAM1,3 neurons in the R30G08 strain left the rewarding effect of all three sugars largely unaffected (Figures 3A–3D); ablating the pPAM1,3,4 neurons in the R58E02 strain reduced only fructose and sorbitol reward learning (Figures 3E–3H); ablating pPAM1–4—that is, all neurons of the cluster—in the R64H06 strain reduced learning for all three sugars (Figures 3I–3L). By a combinatorial argument, the pPAM4 neuron thus appears to be required for the full rewarding effects of fructose and sorbitol, whereas the pPAM2 neuron appears to be required for the full rewarding effect of arabinose (Figure 3R; "labeled line hypothesis"). However, acute silencing of synaptic output from pPAM2 neurons does not impair the rewarding effect of arabinose (Figures 4C–4H). It therefore seems possible that ablating progressively more pPAM neurons leads to more severe reductions in sugar reward learning (Figures 4A and 4B; "mass action hypothesis"). In any event, in none of the cases of defective odor-reward learning did we find gross defects in task-relevant sensory-motor abilities (Figures S3A–S3E).

We next examined the requirement of pPAM neurons for aversive learning [33–36]. Removal of the pPAM1,3,4 neurons

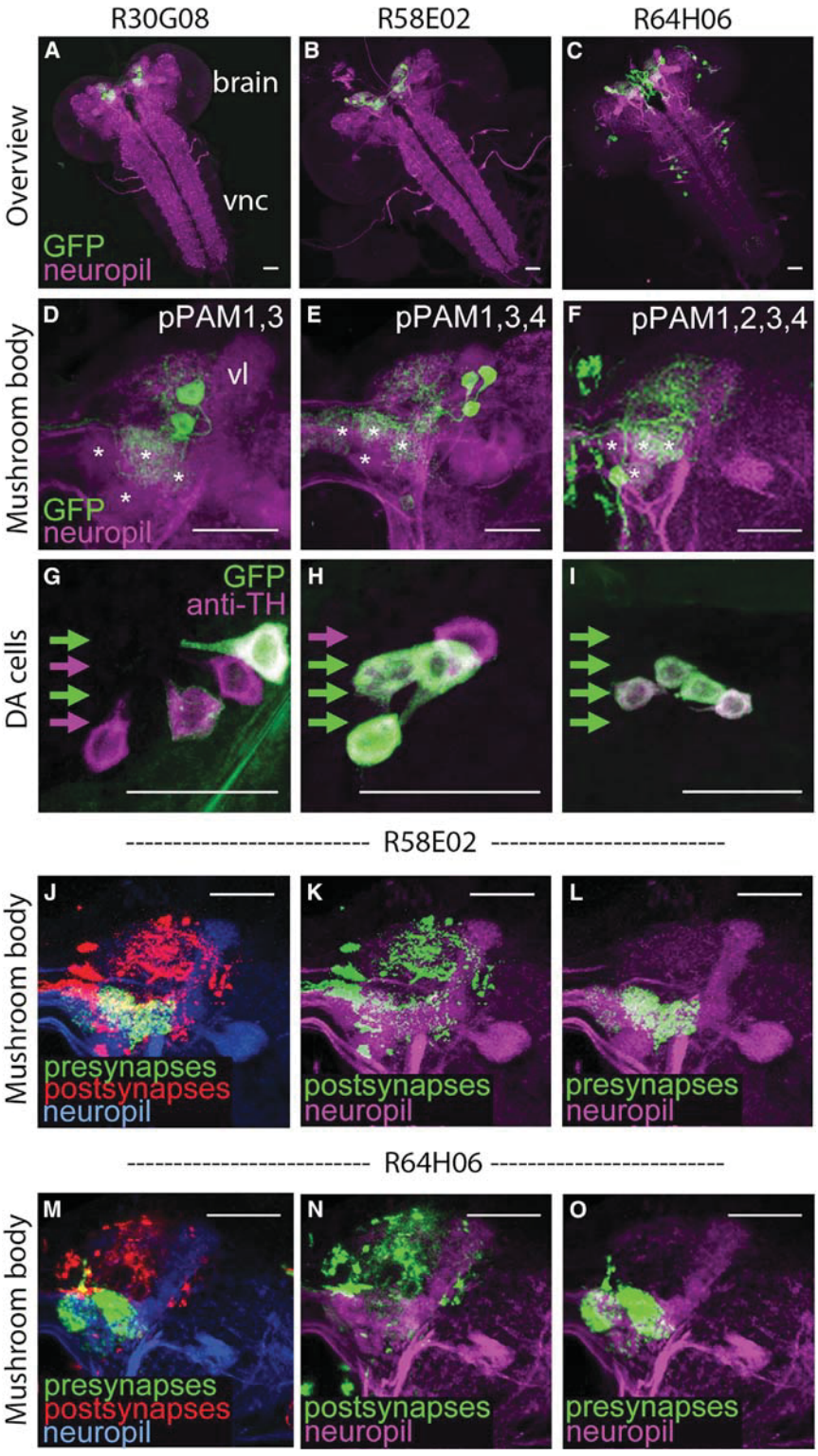

Figure 2. Gal4 Strains Covering pPAM Cluster Neurons

(A, D, and G) The R30G08 driver strain covers two likely dopaminergic TH-positive neurons, namely pPAM1,3.

(A and D) The R30G08 driver strain was crossed to the UAS-*mCD8::GFP* effector strain. A z projection of an anterior view of a larval whole-mount brain is shown using anti-GFP (green) and, as neuropil/axonal tract markers, anti-ChAT/FasII (magenta). The pPAM1,3 neurons are identified based on expression in their respective tiles of the medial lobe and by flp-out clones (Figure S1 shows one of the rare flp-out clones of pPAM2). Asterisks in (D) highlight the four different subunits of the medial lobe (same in E and F).

(G) Same genotype as above. Co-labeling of anti-*GFP* and anti-*TH* suggests a likely dopaminergic nature of the pPAM1,3 neurons covered by the R30G08 driver strain.

(B, E, and H) The R58E02 driver strain covers three likely dopaminergic TH-positive neurons, namely pPAM1,3,4. Other details are as above. Supporting flp-out clones are shown in Figure S1 (Figure S1 shows one of the rare flp-out clones of pPAM2).

(C, F, and I) The R64H06 driver strain covers all four likely dopaminergic TH-positive pPAM1–4 neurons. Note the innervation of the complete medial lobe. Other details are as above. Supporting flp-out clones are displayed in Figure S1.

(J–O) Polarity of the pPAM cluster neurons.

(J and M) With R58E02 (J) and R64H06 (M) used as driver strains, UAS-*DenMark* was expressed to mark postsynaptic, input regions (red) and UAS-*nsyb::GFP* to mark presynaptic, output regions (green). Anti-ChAT/FasII neuropil staining is shown in blue.

(K and N) The postsynaptic, input regions (shown in green; neuropil and axonal tracts are shown in magenta) of the pPAM neurons are mainly located in the medial and lateral protocerebrum, with additional sparse signals from the medial lobe.

(L and O) The presynaptic, output regions (shown in green; neuropil and axonal tracts are shown in magenta) are limited to the medial lobe of the mushroom body.

Scale bars, 50 μm (A–C) and 25 μm (D–O). See also Figure S1.

using the driver strain R58E02 had no effect on odor-quinine memory scores (Figure 3M). Use of the driver strain R64H06 that covers all pPAM neurons confirms this result (Figure 3P). Thus, the pPAM neurons appear dispensable for odor-quinine learning.

We further examined the effects of acutely blocking synaptic output from the pPAM neurons. We expressed a temperature-sensitive dynamin (Shibire^{ts}) in the pPAM1,3,4 neurons to block their synaptic output only during the experiment; this is sufficient to reveal their acute requirement for appetitive learning using fructose as sugar reward (Figure 3N). This manipulation left task-relevant sensory-motor function intact (Figures S3F–S3H).

To test whether the impairment in fructose reward learning upon disabling the pPAM neurons is related to dopamine function, we knocked down the dopamine-synthetizing TH enzyme

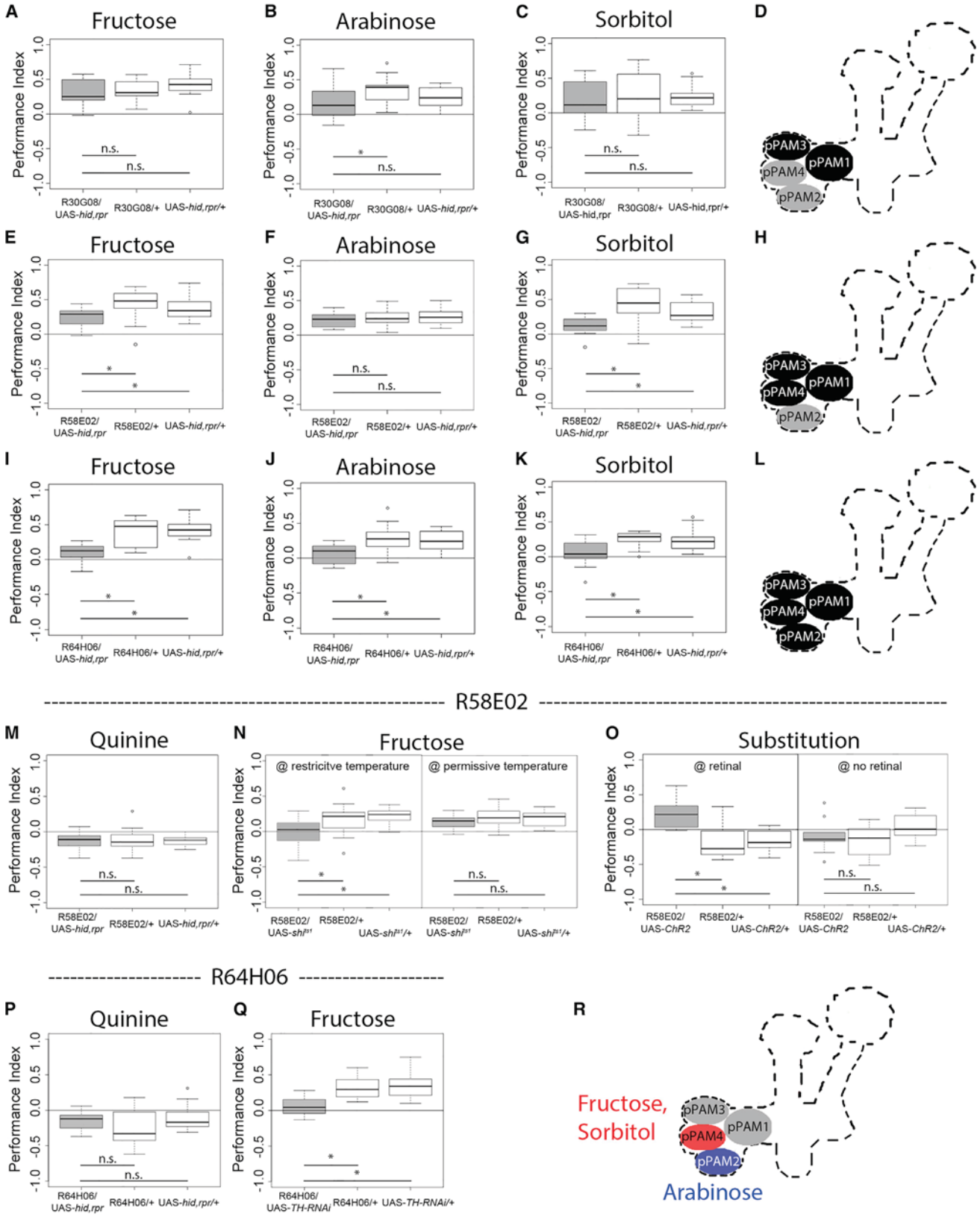

Figure 3. pPAM Neurons Mediate Reward Signals

In all panels (except D, H, L, and R), associative performance indices are shown for tests immediately after associative, classical conditioning. The three pPAM-specific driver strains R30G08, R58E02, and R64H06 were crossed to the effector UAS-*hid,rpr* to induce apoptosis (A–M and P), to UAS-*shi*^{ts} to acutely block

(legend continued on next page)

by RNAi, using the driver R64H06 covering all pPAM neurons. This manipulation led to a reduction in fructose reward learning (Figure 3Q), whereas task-relevant sensory-motor function remained intact (Figures S3I–S3K). This result also makes it unlikely that non-pPAM neurons covered in R64H06 contribute to the phenotype, as these do not express TH.

Based on the results so far, we suspected that optogenetic activation of pPAM neurons by transgenic Channelrhodopsin2 expression might substitute for reward stimulation [8]. Activation of the pPAM1,3,4 neurons as covered by the R58E02 driver was sufficient for such reward substitution (Figure 3O, left), provided that retinal was fed to the larvae to enable Channelrhodopsin2 function (Figure 3O, right). Notably, this rewarding effect was strong enough to overcome the otherwise slightly punitive effect of the light needed to activate Channelrhodopsin2 (see genetic controls in Figure 3O).

We conclude that the pPAM neurons mediate a likely dopaminergic appetitive reinforcement signal toward the mushroom body.

Reinforcement Signaling in Larval *Drosophila*

Our discovery of the four paired pPAM neurons as mediators of an appetitive reinforcement signal in larval *Drosophila* complements earlier work showing that a distinct set of likely dopaminergic neurons, included in the TH-Gal4 expression pattern, is sufficient as an aversive reinforcement signal in these animals [8]. Such division of labor uncovers an organizational principle shared with adult *Drosophila*, though at massively reduced cell numbers, a principle that may hold true in mammals, as well [1–4, 7, 9, 10, 37] (but see [6]).

Given that all four pPAM neurons innervate the medial lobes of the mushroom bodies, our study points to the medial lobe as site of odor-reward memory trace formation. Regarding aversive learning, the likely dopaminergic inputs to other regions could provide this function [5]. This situation, again at much reduced cell numbers, uncovers a principle shared with adult *Drosophila* (Figure S4) [1–4, 10, 15, 38, 39].

Likewise similar to the situation in adults [2], activation of a set of likely octopaminergic/tyraminergic neurons is sufficient to mediate an appetitive reinforcement effect, too [8]. In honeybees, activation of a single, unpaired and likely octopaminergic neuron, the VUM_{mx1} neuron, is sufficient to signal appetitive reinforcement [40]. Within the mushroom body, this neuron innervates the olfactory input regions in the calyx. A similar type of neuron exists in adult and larval *Drosophila* [41, 42]. The way in which the dopaminergic and the octopaminergic/tyraminergic systems jointly organize appetitive reinforcement signaling is a fascinating issue. These systems may differentially convey nutritional and non-nutritional aspects of reward and/or different kinds of reward [2, 11, 31, 41, 43].

Thus, reinforcement processing in the larval and the adult *Drosophila* brain follows similar principles of circuit organization—however, with strikingly reduced cell numbers in the larval case. The larval pPAM cluster features only four neurons, whereas in the adult there are about 30 times more of these neurons [1, 2, 15]. Although this may allow for the representation of more kinds of "valuables" in the adult (Figure S4) [11, 44, 45], the numerical simplicity of the larval nervous system, together with the ongoing efforts toward its complete connectome [19], might bring a full-brain, single-cell, and single-synapse understanding of memory into reach for the larva.

EXPERIMENTAL PROCEDURES

Fly Strains

Flies were reared under standard conditions unless mentioned otherwise. UAS-*mCD8::GFP* (*w*;;P{20XUAS-IVS-mCD8::GFPattP2*; Bloomington Stock

synaptic output (N), to UAS-*ChR2* to artificially activate them (O), or to UAS-TH-RNAi to knock down TH function (Q). Box plots represent the median as the middle line and 25%/75% and 10%/90% as box boundaries and whiskers, respectively. Sample size in each case is n = 16. Differences between groups are depicted below the respective box plots. Small circles indicate outliers. n.s., $p > 0.05$; *$p < 0.05$.

(A–C) With R30G08 used as driver strain to ablate the pPAM1,3 neurons, associative performance indices are not robustly decreased for any of the three sugar rewards. That is, in no case were associative performance indices upon pPAM1,3 ablation lower than in both genetic controls.

(D) Schematic of medial lobe innervation by the pPAM1,3 neurons. Solid fill indicates the ablation, and light fill indicates the presence of the cell innervating the respective tile.

(E–G) Using R58E02 as driver strain to ablate the pPAM1,3,4 neurons leads to an impairment in odor-fructose (both $p < 0.05$) and odor-sorbitol (both $p < 0.05$) learning, but not for arabinose as reward (both $p > 0.05$).

(H) Schematic of medial lobe innervation by the pPAM1,3,4 neurons.

(I–K) Ablation of all four pPAM neurons using R64H06 as a driver strain leads to an impairment for all three sugar rewards (all $p < 0.05$).

(L) Schematic of medial lobe innervation by the pPAM1–4 neurons.

(M) Aversive olfactory learning using quinine as punishment is not decreased upon ablation of pPAM1,3,4 using R58E02 as driver (all $p > 0.05$).

(N) To test for the acute function of the pPAM1,3,4 neurons, we expressed a temperature-sensitive dynamin using UAS-shi^{ts1} from the R58E02 driver. An acute block of synaptic output from these neurons, at restrictive temperature, strongly reduces odor-fructose associative function (both $p < 0.05$). At a permissive temperature, synaptic output remains intact in the experimental and the control genotypes, and no difference in associative function is detectable between strains (both $p > 0.05$).

(O) To test whether optogenetic activation of the pPAM1,3,4 neurons is sufficient to substitute for a reward, we used the R58E02 driver in combination with UAS-*ChR2* to express Channelrhodopsin2. The behavioral experiment then is the same as above, except that the sugar reward is replaced by light-activation of the pPAM1,3,4 neurons. That is, one odor is presented together with light stimulation and thus with activation of pPAM1,3,4, whereas the second odor is presented in darkness. Only larvae of the experimental genotype, but not of the genetic controls, show an associative difference in preference between these groups (left; @ retinal; both $p < 0.05$). This shows that activation of the pPAM1,3,4 neurons is sufficient to mediate a reward signal. Without feeding retinal, which is required for Channelrhodopsin2 function, no such appetitive learning is observed in any genotype (right; @ no retinal; both $p > 0.05$).

(P) Aversive olfactory learning using quinine as punishment is not decreased even upon ablation of the entire pPAM cluster using R64H06 as driver (both $p > 0.05$).

(Q) Knockdown of TH function in all four pPAM neurons using R64H06 as driver strain leads to impaired learning using fructose as a reward (both $p < 0.05$).

(R) Labeled line hypothesis. The defects in associative function upon ablating subsets of pPAM neurons as shown in Figure 3 could be explained by a combinatorial argument suggesting that pPAM4 is essential for a fructose/sorbitol reward signal, whereas pPAM2 is essential for an arabinose reward signal.

See also Figures S2, S3, and S4.

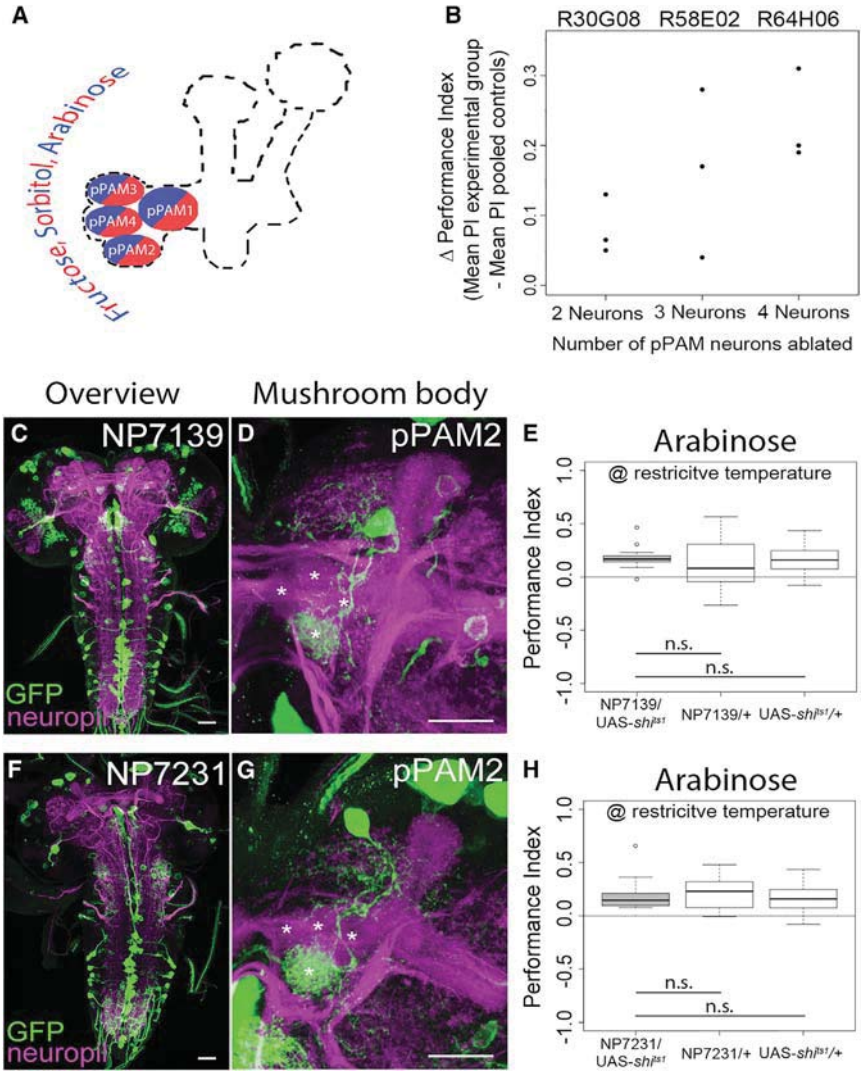

Figure 4. Alternative Hypothesis of Reward Processing in the pPAM Neurons

(A) Mass action hypothesis. The number, rather than the identity, of pPAM neurons may matter for reward function, such that defects in associative function are the more likely to be observed the more pPAM neurons are affected. The figure illustrates that all pPAM neurons may thus be involved in mediating the reward function of all three sugars.

(B) Semi-schematical presentation of the decrease in associative function upon ablating two pPAM neurons (in R30G08), three pPAM neurons (in R58E02), or all four pPAM neurons (in R64H06); each data point refers to the median performance index (PI) for either one of the three sugars. This plot suggests that defects get stronger the more pPAM neurons are ablated.

(C–H) Within the mushroom bodies, the driver strains NP7139 and NP7231 cover only the pPAM2 neuron. (C, D, F, and G) Driver strains were crossed to the UAS-*mCD8::GFP* effector strain. z projections are shown, either of the entire brain (C and F) or of the mushroom body (D and G), with an anterior view using anti-GFP (green) and, as neuropil/axonal tract markers, anti-ChAT/FasII (magenta). Use of NP7139 (C–E) or NP7231 (F–H) as driver strains to block synaptic output from the pPAM2 neuron does not impair learning with arabinose as reward (all $p > 0.05$); this does not support the labeled line hypothesis (Figure 3R). Asterisks highlight the four different subunits of the medial lobe in (D) and (G). Box plots represent the median as the middle line and 25%/75% and 10%/90% as box boundaries and whiskers, respectively. Scale bars, 25 μm (C, D, F, and G).

Center no. 32194) and *y, w, hsp70-flp*; *Sp/CyO*; UAS>*CD2y*$^{+}$>*mCD8::GFP/TM6b* [24] were used to analyze the morphology of the pPAM cluster. UAS-*nsyb::GFP;* UAS-*DenMark* (*w*^{1118}*; L1/CyO; P{UAS-DenMark}3, P{UAS-syt.eGFP}3*; Bloomington Stock Center no. 33065) was used to label pre- and postsynaptic terminals [26]. The Gal4 strains R30G08/TM6b, R58E02, and R64H06/TM6b (*w*^{1118}*; P{GMR30G08-GAL4}attP2/TM6; w*^{1118}*; P{GMR58E02-GAL4}attP2; w*^{1118}*; P{GMR64H06-GAL4}attP2/TM6*; Bloomington Stock Center nos. 48101, 41347, 49608) were identified by screening the database of [23]. The Gal4 strains NP7139 and NP7231 (*w[*] P{w[+mW.hs] = GawB}*; Kyoto Stock Center nos. 114098 and 114162) were identified by screening the NP collection. UAS-*hid,rpr*; (*y, w*^{1118}*, P{UAS-hid}, P{UAS-rpr}*) was used to ablate neurons [28, 29, 46]; UAS-*shi*^{ts} (*w*^{1118}*; P{UAS-shi*^{ts1}*};* Bloomington Stock Center no. 44222) [47] was used to acutely block synaptic output; and UAS-*ChR2* (*w**;;*P{UAS-ChR2.S}3*; Bloomington Stock Center no. 9681) allows activation of neurons by blue light [8]. UAS-TH-RNAi was used to interfere specifically with TH gene function (TriP JF01813; Bloomington Stock Center no. 25796) [48]. The strains were not isogenized before the experiments.

Immunostaining

Third-instar larvae were put on ice and dissected in PBS [5, 41]. Brains were fixed in 3.6% formaldehyde (Merck) in PBS for 30 min. After eight rinses in PBT (PBS with 3% Triton X-100; Sigma-Aldrich), brains were blocked with 5% normal goat serum (Vector Laboratories) in PBT for 2 hr and incubated for 2 days with primary antibodies at 4°C. Before application of the secondary antibodies for 2 days at 4°C, brains were washed eight times with PBT. After secondary antibody incubation, brains were washed eight times with PBT, mounted in Vectashield (Vector Laboratories) and stored at 4°C in darkness. Images were taken with a Zeiss LSM 510M confocal microscope with 25× or 40× glycerol objectives. The resulting image stacks were projected and analyzed with Image J (NIH; http://imagej.nih.gov/ij). Contrast and brightness adjustment, rotation, and arrangement of images were performed in Photoshop (Adobe Systems).

For the single-cell staining *y, w, hsp70-flp*; *Sp/CyO*; UAS>*CD2y*$^{+}$>*mCD8::GFP/TM6b* virgins were crossed to R30G08, R58E02, or R64H06 males. A single heat shock of 37°C was applied for 18 min by placement of the vials in a water bath. For the onset of heat shock, we chose different times from 0 to 200 hr after egg laying.

Antibodies

For analysis of Gal4 expression patterns and individual neurons a rabbit anti-GFP antibody (A6455; Molecular Probes; 1:1000) and two different mouse antibodies for staining the cholinergic neuropil (ChAT4B1; DSHB; 1:150) and axonal tracts (1d4 anti-FasciclinII; DSHB; 1:50) were applied [5, 41]. DA neurons were visualized with a polyclonal antibody against TH (1:800) [5]. Pre- and postsynaptic structures were identified using the conjugated goat GFP FITC antibody (ab 6662; Abcam; 1:1000) to label the UAS-*nsyb::GFP* effector and rabbit anti-DsRed (632496; Clonetech; 1:200) to visualize the UAS-*DenMark* effector.

As secondary antibodies, goat anti-rabbit IgG Alexa Fluor 488 (A11008; Molecular Probes; 1:200), goat anti-mouse IgG Alexa Fluor 647 (A21235; Molecular Probes; 1:200), goat anti-mouse IgG Cy3 (A10521; Molecular Probes; 1:200) and goat anti-rabbit IgG Cy5 (A10523; Molecular Probes; 1:200) were used.

Odor-Sugar Learning

Experiments were conducted on assay plates filled with a thin layer of 2.5% agarose containing either pure agarose (Sigma Aldrich cat. no. A5093; CAS no. 9012-36-6) or agarose plus D-fructose (Sigma Aldrich cat. no. 47740; CAS no. 57-48-7), D-arabinose (Sigma Aldrich cat. no. A3131; CAS no. 10323-20-3), or D-sorbitol (Sigma Aldrich cat. no. W302902; CAS no. 50-70-4) at a concentration of 2 M [30, 31]. As olfactory stimuli, we used 10 μl amyl acetate (AM; Fluka 46022; CAS no. 628-63-7; diluted 1:250 in paraffin oil, Fluka 76235; CAS no. 8012-95-1) and benzaldehyde (BA; undiluted; Fluka 12010; CAS no. 100-52-7). Odorants were loaded into custom-made Teflon containers (4.5 mm diameter) with perforated lids [30]. A first group of 30 animals was exposed to AM while crawling on agarose medium containing in addition sugar as a positive reinforcer. After 5 min, larvae were transferred to a fresh, pure-agarose Petri dish and exposed to BA (AM+/BA). This cycle of training trials was repeated two more times. A second group of larvae received reciprocal training (AM/BA+). Then larvae were transferred onto test plates containing pure agarose on which AM and BA were presented on opposite sides. After 5 min, individuals were counted as located on the AM side (# AM), the BA side (# BA), or in a 10 mm neutral zone. We determined a preference index for each training group as follows (these preference indices are documented in Figure S2):

$$\mathrm{Pref}_{AM+/BA} = (\#\,AM - \#\,BA)/\#\,Total \qquad \text{(Equation 1A)}$$

$$\mathrm{Pref}_{AM/BA+} = (\#\,AM - \#\,BA)/\#\,Total \qquad \text{(Equation 1B)}$$

To measure specifically the effect of associative learning, we then calculated the associative performance index (PI) as the difference in preference between the reciprocally trained larvae:

$$PI = \left(\mathrm{Pref}_{AM+/BA} - \mathrm{Pref}_{AM/BA+}\right)/2 \qquad \text{(Equation 2)}$$

Negative PIs thus represent aversive associative learning, whereas positive PIs indicate appetitive associative learning. Division by 2 ensures scores are bound within (−1; 1). The sequence of training trials (i.e., AM+/BA or BA/AM+) was alternated across repetitions of the experiment.

Odor-Quinine Learning

Odor-quinine learning was performed as described above for odor-sugar learning [33], except that instead of sugar 6 mM quinine (quinine-hemisulfate; Sigma Aldrich cat. no. Q1250; CAS no. 207671-44-1) was used with 1% agarose [49]. Given that learned aversive behavior is a form of learned escape, the testing situation needs to actually warrant escape; therefore, quinine needs to be added to the test plate [33].

Substitution Experiment

To substitute an actual sugar reward by remotely activating neurons, we used UAS-*ChR2* [8]. Fly strains were reared on standard *Drosophila* medium that included retinal (100 mM final concentration; Sigma Aldrich cat. no. R2500; CAS no. 116-31-4) at 25°C in darkness. A group of 30 feeding-stage third-instar larvae were placed onto plates containing 2.5% agarose and exposed to either AM or BA. During the presentation of the first odor, the larvae were exposed to blue light (470 nm; ~20 000 lux) for 5 min. The second odor was then presented in darkness. As described for odor-sugar learning, training was performed reciprocally and the sequence of training trials was alternated across repetitions of the experiment. Data were then scored as above.

Acutely Blocking Synaptic Output with *shibire^{ts}*

To acutely block synaptic output, we used UAS-*shi^{ts}* [47]. The larvae were incubated for 2 min in a water bath at 37°C. The behavioral experiments were then performed as described before, at a restrictive temperature of about 35°C. Control experiments were performed with incubation at room temperature and at a permissive temperature of about 23°C.

Statistical Methods

Kruskal-Wallis tests were performed and, in case of significance, followed by Wilcoxon rank-sum tests; Holm-Bonferroni corrections were used for multiple comparisons as applicable. Likewise, Wilcoxon signed-ranked tests were used to compare values against chance level.

All statistical analyses were performed with R version 2.14.0 and Windows Excel 2010. Figure alignments were done with Adobe Photoshop. The behavioral data are presented as boxplots (middle line, median; box boundaries, 25%/75% quantiles; whiskers, 10%/90% quantiles; circles, outliers). Asterisks and "n.s." indicate $p > 0.05$ and $p < 0.05$, respectively.

SUPPLEMENTAL INFORMATION

Supplemental Information includes Supplemental Experimental Procedures and four figures and can be found with this article online

AUTHOR CONTRIBUTIONS

Conceptualization, A.R, N.L.W, N.Y., M.Z, J.W.T., H.T., T.S., B.G., and A.S.T; Methodology, A.R., N.L.W., M.Z., J.W.T., H.T., T.S., B.G., and A.S.T; Investigation, A.R., N.L.W., B.S., A.H., and A.S.T., Writing, A.R., N.Y., M.Z., J.W.T., H.T., T.S., B.G., and A.S.T; Supervision, A.R., M.Z., J.W.T., H.T., B.G., and A.S.T.

ACKNOWLEDGMENTS

This work was supported by the Deutsche Forschungsgemeinschaft (TH1584/1-1 and TH1584/3-1 to A.S.T.; CRC 779 Motivated behavior to B.G.), the Swiss National Science Foundation (31003A132812/1 to A.S.T.), the Baden Württemberg Stiftung (to A.S.T.), the Bioimaging Center and Zukunftkolleg of the University of Konstanz (to A.S.T.), the Bundesministerium für Bildung and Forschung (Bernstain Focus Program Insect-Inspired Robotics to B.G.), and the European Commission (MINIMAL FP7 - 618045 to B.G.). We thank Yoshihiro Aso, Reinhard F. Stocker, Michael Schleyer, Ayse Yarali, Dennis Pauls, Mareike Selcho, and Wolf Hütteroth for discussions and comments. Additionally, we thank Lyubov Pankevych and Margarete Ehrenfried for fly care and maintenance.

REFERENCES

1. Liu, C., Plaçais, P.Y., Yamagata, N., Pfeiffer, B.D., Aso, Y., Friedrich, A.B., Siwanowicz, I., Rubin, G.M., Preat, T., and Tanimoto, H. (2012). A subset of dopamine neurons signals reward for odour memory in Drosophila. Nature *488*, 512–516.
2. Burke, C.J., Huetteroth, W., Owald, D., Perisse, E., Krashes, M.J., Das, G., Gohl, D., Silies, M., Certel, S., and Waddell, S. (2012). Layered reward signalling through octopamine and dopamine in Drosophila. Nature *492*, 433–437.
3. Schwaerzel, M., Monastirioti, M., Scholz, H., Friggi-Grelin, F., Birman, S., and Heisenberg, M. (2003). Dopamine and octopamine differentiate between aversive and appetitive olfactory memories in Drosophila. J. Neurosci. *23*, 10495–10502.
4. Aso, Y., Herb, A., Ogueta, M., Siwanowicz, I., Templier, T., Friedrich, A.B., Ito, K., Scholz, H., and Tanimoto, H. (2012). Three dopamine pathways induce aversive odor memories with different stability. PLoS Genet. *8*, e1002768.
5. Selcho, M., Pauls, D., Han, K.A., Stocker, R.F., and Thum, A.S. (2009). The role of dopamine in Drosophila larval classical olfactory conditioning. PLoS ONE *4*, e5897.

6. Schultz, W. (2013). Updating dopamine reward signals. Curr. Opin. Neurobiol. *23*, 229–238.
7. Matsumoto, M., and Hikosaka, O. (2009). Two types of dopamine neuron distinctly convey positive and negative motivational signals. Nature *459*, 837–841.
8. Schroll, C., Riemensperger, T., Bucher, D., Ehmer, J., Völler, T., Erbguth, K., Gerber, B., Hendel, T., Nagel, G., Buchner, E., and Fiala, A. (2006). Light-induced activation of distinct modulatory neurons triggers appetitive or aversive learning in Drosophila larvae. Curr. Biol. *16*, 1741–1747.
9. Nitsche, M.A., Kuo, M.F., Grosch, J., Bergner, C., Monte-Silva, K., and Paulus, W. (2009). D1-receptor impact on neuroplasticity in humans. J. Neurosci. *29*, 2648–2653.
10. Aso, Y., Sitaraman, D., Ichinose, T., Kaun, K.R., Vogt, K., Belliart-Guérin, G., Plaçais, P.Y., Robie, A.A., Yamagata, N., Schnaitmann, C., et al. (2014). Mushroom body output neurons encode valence and guide memory-based action selection in Drosophila. eLife *3*, e04580.
11. Yamagata, N., Ichinose, T., Aso, Y., Plaçais, P.Y., Friedrich, A.B., Sima, R.J., Preat, T., Rubin, G.M., and Tanimoto, H. (2015). Distinct dopamine neurons mediate reward signals for short- and long-term memories. Proc. Natl. Acad. Sci. USA *112*, 578–583.
12. Masek, P., Worden, K., Aso, Y., Rubin, G.M., and Keene, A.C. (2015). A dopamine-modulated neural circuit regulating aversive taste memory in Drosophila. Curr. Biol. *25*, 1535–1541.
13. Larsen, C., Shy, D., Spindler, S.R., Fung, S., Pereanu, W., Younossi-Hartenstein, A., and Hartenstein, V. (2009). Patterns of growth, axonal extension and axonal arborization of neuronal lineages in the developing Drosophila brain. Dev. Biol. *335*, 289–304.
14. Tomer, R., Denes, A.S., Tessmar-Raible, K., and Arendt, D. (2010). Profiling by image registration reveals common origin of annelid mushroom bodies and vertebrate pallium. Cell *142*, 800–809.
15. Aso, Y., Hattori, D., Yu, Y., Johnston, R.M., Iyer, N.A., Ngo, T.T., Dionne, H., Abbott, L.F., Axel, R., Tanimoto, H., and Rubin, G.M. (2014). The neuronal architecture of the mushroom body provides a logic for associative learning. eLife *3*, e04577.
16. Python, F., and Stocker, R.F. (2002). Adult-like complexity of the larval antennal lobe of D. melanogaster despite markedly low numbers of odorant receptor neurons. J. Comp. Neurol. *445*, 374–387.
17. Stocker, R.F. (2008). Design of the larval chemosensory system. Adv. Exp. Med. Biol. *628*, 69–81.
18. Gerber, B., and Stocker, R.F. (2007). The Drosophila larva as a model for studying chemosensation and chemosensory learning: a review. Chem. Senses *32*, 65–89.
19. Ohyama, T., Schneider-Mizell, C.M., Fetter, R.D., Aleman, J.V., Franconville, R., Rivera-Alba, M., Mensh, B.D., Branson, K.M., Simpson, J.H., Truman, J.W., et al. (2015). A multilevel multimodal circuit enhances action selection in Drosophila. Nature *520*, 633–639.
20. Friggi-Grelin, F., Coulom, H., Meller, M., Gomez, D., Hirsh, J., and Birman, S. (2003). Targeted gene expression in Drosophila dopaminergic cells using regulatory sequences from tyrosine hydroxylase. J. Neurobiol. *54*, 618–627.
21. Budnik, V., Martin-Morris, L., and White, K. (1986). Perturbed pattern of catecholamine-containing neurons in mutant Drosophila deficient in the enzyme dopa decarboxylase. J. Neurosci. *6*, 3682–3691.
22. Blanco, J., Pandey, R., Wasser, M., and Udolph, G. (2011). Orthodenticle is necessary for survival of a cluster of clonally related dopaminergic neurons in the Drosophila larval and adult brain. Neural Dev. *6*, 34.
23. Li, H.H., Kroll, J.R., Lennox, S.M., Ogundeyi, O., Jeter, J., Depasquale, G., and Truman, J.W. (2014). A GAL4 driver resource for developmental and behavioral studies on the larval CNS of Drosophila. Cell Rep. *8*, 897–908.
24. Wong, A.M., Wang, J.W., and Axel, R. (2002). Spatial representation of the glomerular map in the Drosophila protocerebrum. Cell *109*, 229–241.
25. Niewalda, T., Jeske, I., Michels, B., and Gerber, B. (2014). 'Peer pressure' in larval Drosophila? Biol. Open *3*, 575–582.
26. Nicolaï, L.J., Ramaekers, A., Raemaekers, T., Drozdzecki, A., Mauss, A.S., Yan, J., Landgraf, M., Annaert, W., and Hassan, B.A. (2010). Genetically encoded dendritic marker sheds light on neuronal connectivity in Drosophila. Proc. Natl. Acad. Sci. USA *107*, 20553–20558.
27. Ito, K., Suzuki, K., Estes, P., Ramaswami, M., Yamamoto, D., and Strausfeld, N.J. (1998). The organization of extrinsic neurons and their implications in the functional roles of the mushroom bodies in Drosophila melanogaster Meigen. Learn. Mem. *5*, 52–77.
28. Abbott, M.K., and Lengyel, J.A. (1991). Embryonic head involution and rotation of male terminalia require the Drosophila locus head involution defective. Genetics *129*, 783–789.
29. White, K., Tahaoglu, E., and Steller, H. (1996). Cell killing by the Drosophila gene reaper. Science *271*, 805–807.
30. Scherer, S., Stocker, R.F., and Gerber, B. (2003). Olfactory learning in individually assayed Drosophila larvae. Learn. Mem. *10*, 217–225.
31. Rohwedder, A., Pfitzenmaier, J.E., Ramsperger, N., Apostolopoulou, A.A., Widmann, A., and Thum, A.S. (2012). Nutritional value-dependent and nutritional value-independent effects on Drosophila melanogaster larval behavior. Chem. Senses *37*, 711–721.
32. Schipanski, A., Yarali, A., Niewalda, T., and Gerber, B. (2008). Behavioral analyses of sugar processing in choice, feeding, and learning in larval Drosophila. Chem. Senses *33*, 563–573.
33. Gerber, B., and Hendel, T. (2006). Outcome expectations drive learned behaviour in larval Drosophila. Proc. Biol. Sci. *273*, 2965–2968.
34. Honjo, K., and Furukubo-Tokunaga, K. (2009). Distinctive neuronal networks and biochemical pathways for appetitive and aversive memory in Drosophila larvae. J. Neurosci. *29*, 852–862.
35. Apostolopoulou, A.A., Mazija, L., Wüst, A., and Thum, A.S. (2014). The neuronal and molecular basis of quinine-dependent bitter taste signaling in Drosophila larvae. Front. Behav. Neurosci. *8*, 6.
36. Schleyer, M., Saumweber, T., Nahrendorf, W., Fischer, B., von Alpen, D., Pauls, D., Thum, A., and Gerber, B. (2011). A behavior-based circuit model of how outcome expectations organize learned behavior in larval Drosophila. Learn. Mem. *18*, 639–653.
37. Perisse, E., Burke, C., Huetteroth, W., and Waddell, S. (2013). Shocking revelations and saccharin sweetness in the study of Drosophila olfactory memory. Curr. Biol. *23*, R752–R763.
38. Aso, Y., Siwanowicz, I., Bräcker, L., Ito, K., Kitamoto, T., and Tanimoto, H. (2010). Specific dopaminergic neurons for the formation of labile aversive memory. Curr. Biol. *20*, 1445–1451.
39. Claridge-Chang, A., Roorda, R.D., Vrontou, E., Sjulson, L., Li, H., Hirsh, J., and Miesenböck, G. (2009). Writing memories with light-addressable reinforcement circuitry. Cell *139*, 405–415.
40. Hammer, M. (1993). An identified neuron mediates the unconditioned stimulus in associative olfactory learning in honeybees. Nature *366*, 59–63.
41. Selcho, M., Pauls, D., Huser, A., Stocker, R.F., and Thum, A.S. (2014). Characterization of the octopaminergic and tyraminergic neurons in the central brain of Drosophila larvae. J. Comp. Neurol. *522*, 3485–3500.
42. Busch, S., Selcho, M., Ito, K., and Tanimoto, H. (2009). A map of octopaminergic neurons in the Drosophila brain. J. Comp. Neurol. *513*, 643–667.
43. Schleyer, M., Miura, D., Tanimura, T., and Gerber, B. (2015). Learning the specific quality of taste reinforcement in larval Drosophila. eLife *4*, e04711.
44. Huetteroth, W., Perisse, E., Lin, S., Klappenbach, M., Burke, C., and Waddell, S. (2015). Sweet taste and nutrient value subdivide rewarding dopaminergic neurons in Drosophila. Curr. Biol. *25*, 751–758.
45. Lin, S., Owald, D., Chandra, V., Talbot, C., Huetteroth, W., and Waddell, S. (2014). Neural correlates of water reward in thirsty Drosophila. Nat. Neurosci. *17*, 1536–1542.

46. Huser, A., Rohwedder, A., Apostolopoulou, A.A., Widmann, A., Pfitzenmaier, J.E., Maiolo, E.M., Selcho, M., Pauls, D., von Essen, A., Gupta, T., et al. (2012). The serotonergic central nervous system of the Drosophila larva: anatomy and behavioral function. PLoS ONE *7*, e47518.

47. Kitamoto, T. (2002). Conditional disruption of synaptic transmission induces male-male courtship behavior in Drosophila. Proc. Natl. Acad. Sci. USA *99*, 13232–13237.

48. Riemensperger, T., Issa, A.R., Pech, U., Coulom, H., Nguyễn, M.V., Cassar, M., Jacquet, M., Fiala, A., and Birman, S. (2013). A single dopamine pathway underlies progressive locomotor deficits in a Drosophila model of Parkinson disease. Cell Rep. *5*, 952–960.

49. Apostolopoulou, A.A., Hersperger, F., Mazija, L., Widmann, A., Wüst, A., and Thum, A.S. (2014). Composition of agarose substrate affects behavioral output of Drosophila larvae. Front. Behav. Neurosci. *8*, 11.